Rapid Communications

Magnetic susceptibility of quantum spin systems calculated by sine square deformation: One-dimensional, square lattice, and kagome lattice Heisenberg antiferromagnets

Chisa Hotta*
Department of Basic Science, University of Tokyo, 3-8-1 Komaba, Meguro, Tokyo 153-8902, Japan

Kenichi Asano
Center for Education in Liberal Arts and Sciences, Osaka University, Toyonaka, Osaka 560-0043, Japan

(Received 20 July 2018; revised manuscript received 17 September 2018; published 30 October 2018)

We develop a simple and unbiased numerical method to obtain the uniform susceptibility of quantum many-body systems. When a Hamiltonian is spatially deformed by multiplying it with *a sine-square function* that smoothly decreases from the system center toward the edges, the size-scaling law of the excitation energy is drastically transformed to a rapidly converging one. Then, the local magnetization at the system center becomes nearly size independent; the one obtained for the deformed Hamiltonian of a system length as small as $L \sim 10$ provides the value obtained for the original uniform Hamiltonian of $L \sim 100$. This allows us to evaluate a bulk magnetic susceptibility by using the magnetization at the center by existing numerical solvers without any approximation, parameter tuning, or size-scaling analysis. We demonstrate that the susceptibilities of the spin-1/2 antiferromagnetic Heisenberg chain and square lattice obtained by our scheme at $L \sim 10$ agree within 10^{-3} with exact analytical and numerical solutions for $L = \infty$ down to temperatures of 0.1 times the coupling constant. We apply this method to the spin-1/2 kagome lattice Heisenberg antiferromagnet which is of prime interest in the search for spin liquids.

DOI: 10.1103/PhysRevB.98.140405

Introduction. Computing the thermodynamic properties of a many-body quantum lattice model over a wide range of temperature is a challenging problem, which too often remains unsolved. Prominent examples include quantum spin systems with nontrivial ground states such as spin liquids [1], as found in the kagome lattice antiferromagnet [2] and Kitaev model [3]. Experimentally, much effort has been devoted to measuring the magnetic susceptibility of relevant materials such as $ZnCu_3(OH)_6Cl_2$ [4,5], $BaCu_3V_2O_8(OH)_2$ [6], and κ-ET_2X [7,8], to get the smoking guns of their realization. In real materials, the interesting physics is always found at temperatures (T) much lower than the characteristic interaction J; indeed, the T dependence of susceptibility contains rich information such as whether or not the excitations are gapped, and spinons or Majorana fermions form a Dirac point or a Fermi surface. However, numerical methods such as exact diagonalization (ED) [9] and typicality approaches [10–12] suffer from severe finite-size effects and cannot capture the behavior at $T < J$. The quantum Monte Carlo (QMC) method gives reliable results down to $T \sim 0.1J$ [13,14], but is not applied to most of the above-mentioned nontrivial models because of the sign problem.

The high-temperature series expansion (HTE) [15] serves as a powerful analytical tool complementary to numerics. However, the series in powers of $\beta = 1/k_BT$ extends at most up to β^{16} to β^{19} [16,17], and falls off from the true result at $T \lesssim J$. To further extend a series down to $T \sim J/2$, a numerical linked cluster (NLC) approach has been considered [18], and the entropy method [19] succeeded in interpolating between the $T = 0$ limit and a HTE result for $T > J$. However, these methods are still subtle at present since they are based on some assumptions. For instance, the entropy method requires *a priori* knowledge of the susceptibility near $T = 0$ based on the ground-state information. It is highly desirable to have vice versa, i.e., to extract such low T information from the thermodynamic observables.

Given such a situation, a reliable and practical approach that is valid at any temperature is desperately needed. Here, we propose *a parameter-free* and *unbiased* scheme to obtain susceptibility by making use of a device called sine-square deformation (SSD) [20]. The SSD is a spatial modification of the energy scale of the Hamiltonian. It serves as one of the boundary conditions [21–24], as well as works as a real-space renormalization scheme [25]. It also reveals itself as one of the low-energy effective Hamiltonians in two-dimensional (2D) conformal field theory [26–28]. Moreover, the adiabatic connections between the uniform and SSD Hamiltonian are guaranteed [29].

SSD. We first introduce the SSD Hamiltonian, in which an envelope function $f_{\rm SSD}$ makes the original Hamiltonian $\mathcal{H} = \sum_i [h(\boldsymbol{r}_i) - \mu n(\boldsymbol{r}_i)]$ spatially nonuniform,

$$\mathcal{H}_{\rm SSD} = \sum_i f_{\rm SSD}(\boldsymbol{r}_i)[h(\boldsymbol{r}_i) - \mu n(\boldsymbol{r}_i)], \tag{1}$$

$$f_{\rm SSD}(\boldsymbol{r}_i) = \frac{1}{2}\left[1 + \cos\left(\frac{\pi r_i}{R}\right)\right]. \tag{2}$$

Here, $\boldsymbol{r}_i$ is a coordinate of the lattice site if $h(\boldsymbol{r}_i)$ is an on-site term, and it is a coordinate of the bond if $h(\boldsymbol{r}_i)$ is an intersite interaction or a hopping term. The origin of $\boldsymbol{r}_i$ is at the center

*chisa@phys.c.u-tokyo.ac.jp

of the cluster [30]. In $f_{\rm SSD}(\boldsymbol{r}_i)$, R is chosen to be slightly larger than R_0, the distance from the system center to the farthest edge site. If the Hamiltonian is written in terms of fermionic operators, μ is the chemical potential, and $n(\boldsymbol{r}_i)$ is a particle density. If the Hamiltonian is written in terms of spin operators, then μ and $n(\boldsymbol{r}_i)$ are replaced with magnetization $m(\boldsymbol{r}_i)$ and magnetic field H, respectively. We solve $\mathcal{H}_{\rm SSD}$ and evaluate the expectation values of local quantities $A(\boldsymbol{r}_i)$ for energy eigenstates, which are no longer translationally invariant.

One of our previous findings was that the ground-state physical quantities evaluated at the system center, where $f_{\rm SSD}(\boldsymbol{r}_i) \sim 1$, are nearly independent of the system size N and mimic the values for $N \to \infty$ for the original Hamiltonian [31]. For example, by applying a magnetic field H to quantum magnets, one can compute a magnetization density $\langle m(\boldsymbol{r}_i = 0)\rangle$ for the SSD ground state [31]. Even for system lengths $L \lesssim 20$ ($N = L^d$ for d dimension), we obtain a magnetization curve mimicking the bulk exact solution of the original uniform Hamiltonian within an accuracy of 10^{-4} in 1D [31], and 10^{-3} in 2D [25,32].

Intuitively, deforming a Hamiltonian may mean modifying the physical system itself, but for SSD, this is not the case [25,33]. We have shown earlier that the modified part of the Hamiltonian, $\mathcal{H}_{\rm SSD} - \mathcal{H}$, renormalizes the energy levels of the original $\mathcal{H}$ in a way similar to the poor man's scaling by Wilson [25]. The excitation energy $\epsilon_l(L)$ follows a $1/L^2$ behavior [25,34] and densely populates around $\epsilon = 0$, in sharp contrast to the standard scaling law $1/L$. As a result, by using a system size as small as $L \sim 10$ in the SSD system, one can suppress finite-size effects down to those of the original Hamiltonian for $L \sim 100$.

However, it is not clear whether the whole excited-state spectrum is well preserved by SSD. Here, we show that is the case. As a result, thermodynamic quantities are very accurately calculated, and practically free of size effects.

The local Gibbs ensemble. Consider a lattice consisting of $N = L^d$ sites and deform a Hamiltonian following Eq. (1). By solving $\mathcal{H}_{\rm SSD}$ at finite temperature, obtain the Gibbs ensemble $\langle\cdots\rangle$ of a *local physical quantity defined at the system center* with index c as

$$\langle \hat{A}_c \rangle = \frac{1}{\Xi} \sum_l \langle \psi_l | \hat{A}_c | \psi_l \rangle e^{-\beta E_l}, \tag{3}$$

where $\Xi = \sum_l e^{-\beta E_l}$ is the grand partition function, and ψ_l the many-body wave function with energy E_l. Our main conclusion is that, for fermionic systems, the particle densities at the center $\langle \hat{n}_c \rangle$ for systems sized as small as $N \gtrsim 10$ in 1D and $N \gtrsim 20$ in 2D agree with those for the original Hamiltonians for $N \sim \infty$ within $\sim 10^{-3}$. This conclusion holds also for the magnetization $\langle \hat{m}_c \rangle$ of spin systems. Once energy and particle density, or magnetization, are obtained as *smooth functions of β and μ, or H*, thermodynamic potentials and *all* thermodynamic quantities can be evaluated.

Noninteracting system. Let us first demonstrate the validity of our claim for the quantum $S = 1/2$ XX spin chain, $\mathcal{H} = \sum_i (s_i^x s_{i+1}^x + s_i^y s_{i+1}^y - H s_i^z)$, which is equivalent to a free fermionic chain. By applying a small magnetic field, $H = 0.01$–0.1, we obtain an exact solution of the SSD Hamiltonian for a given L, evaluate $\langle \hat{m}_c \rangle$, and take its derivative to obtain

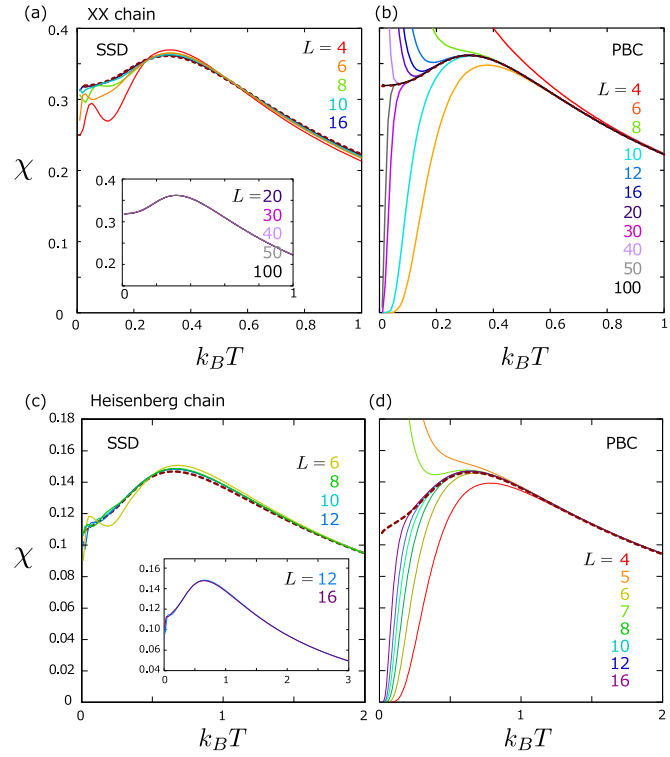

FIG. 1. Susceptibility χ of the 1D XX model, which is equivalent to a free fermionic chain, obtained by (a) our scheme using SSD and (b) the standard method in a uniform system with a periodic boundary condition (PBC). χ of the spin-1/2 Heisenberg chain, obtained by (c) our scheme and (d) the standard method with a PBC. The dashed line is the exact analytical solution for $L = \infty$ [36]. All the results are numerically exact.

a uniform static susceptibility, $\chi = d\langle \hat{m}_c \rangle / dH$. Figure 1(a) shows the result from $L = 6$ up to 100. Already at $L \sim 8$, they are in good agreement with the exact $L = \infty$ susceptibility in the dashed line. Remarkably, the gapless behavior, $\chi > 0$ at $T \to 0$, is correctly obtained even for $L = 4$. When $L \sim 10$, the accuracy of χ already reaches 10^{-3} at $k_B T \sim 0.2$ and 10^{-4} at higher temperatures.

By contrast, χ of the original Hamiltonian obtained in the standard manner, $\chi = -\beta^{-1} \langle (\sum_i m_i)^2 \rangle^2 / N$ (with $H = 0$), suffers from a serious finite-size effect [Fig. 1(b)]. As a consequence of the energy gap in the low-energy spectrum, $\Delta_L \sim O(1/L)$, χ shows an artificial exponential drop, $\propto e^{-\beta \Delta_L}$, at $k_B T \sim 0$.

Heisenberg systems. Our scheme yields similarly high accuracies for interacting systems. For the spin-1/2 Heisenberg chain, $\mathcal{H} = \sum_i s_i s_{i+1} - H \sum_i s_i^z$, we perform a full ED for $L \leqslant 16$ and adopt a typicality approach called the thermal pure quantum (TPQ) method for $L > 16$ [12,35], to solve $\mathcal{H}_{\rm SSD}$. Figure 1(c) shows χ obtained with our scheme. A comparison with the exact solution for $L = \infty$ [36] shows that our results are accurate within the order of 10^{-4} for $L > 10$. Moreover, even for L as small as 8, a small drop of χ appears at temperatures lower than $k_B T \sim 0.01$, reminiscent of the well-known logarithmic singularity in the Bethe ansatz solution [37]. For the original Hamiltonian, finite-size effects

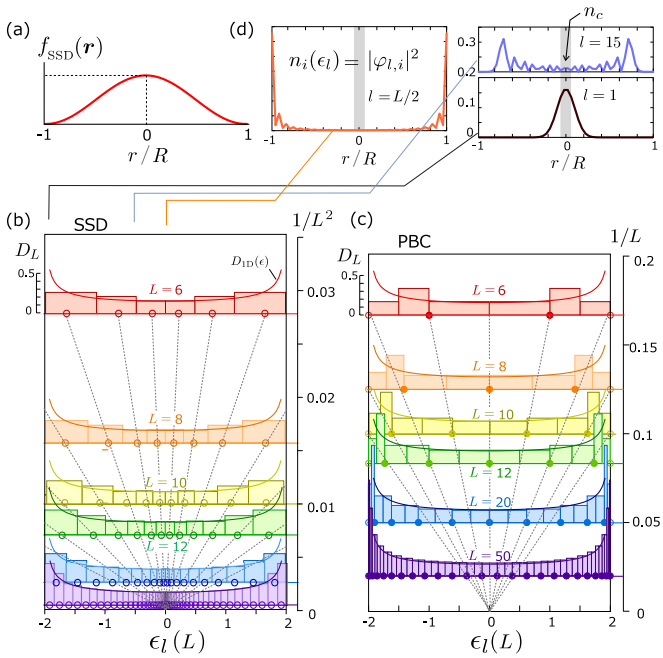

FIG. 2. (a) SSD function $f_{\rm SSD}(\boldsymbol{r})$ in 1D. In (b) and (c), all eigenenergies $\epsilon_l(L)$ of the SSD and original (PBC) free fermionic chain of length $L = 6$, 8, 10, 12, 20 and 50 at $\mu = 0$ are plotted as circles along the horizontal axes shifted vertically by L^{-2} (SSD) and L^{-1} (PBC). The vertical axis on the right-hand side indicates the location of the horizontal axes. Dashed lines show the finite-size-scaling laws, $\epsilon_l(L) \propto L^{-2}$ (SSD) and $\propto L^{-1}$ (PBC). Vertical bars on each horizontal axis show the effective DOS of 1D free fermions $D_L(\epsilon_l)$ evaluated by Eq. (4) as the particle densities of the corresponding eigenstates at the system center divided by the energy spacings. Its scale is given on the left-hand side. Each bar belongs to the circle inside, whereas for doubly degenerate levels marked with solid circles in PBC, the bars on both sides belong to them. Solid lines in (b) and (c) are the bulk exact DOS, $D_{\rm 1D}(\epsilon)$. (d) Spatial distribution of the particle density of the SSD free fermionic chain of $L = 50$ for $l = 25$, 10, and 1, with $l = 1$ being the lowest energy. The shaded values at the center are $n_c(\epsilon_l)$.

again lead to an artificial exponential drop, as shown in Fig. 1(d).

Density of states. We now clarify how the ensemble in Eq. (3) works for a 1D free fermionic chain. Let us deform the Hamiltonian $\mathcal{H} = \sum_i (-c_i^\dagger c_{i+1} + \text{H.c.} - \mu n_i)$ [see Fig. 2(a)] and then diagonalize it into $\mathcal{H}_{\rm SSD} = \sum_l \epsilon_l a_l^\dagger a_l$, where the creation operator $a_l^\dagger$ is related to $c_i^\dagger$ by the unitary transformation $a_l^\dagger = \sum_i \varphi_{l,i} c_i^\dagger$. The distribution of the one-body eigenenergy $\epsilon_l(L)$ ($l = 1$ through L) for system length L is shown in Fig. 2(b). One finds a clear L^{-2} dependence (dashed lines). This is in sharp contrast to the L^{-1} behavior for the original Hamiltonian shown in Fig. 2(c) which is known from the conformal field theory for 1D quantum critical systems [38].

The lth one-body eigenstate has a particle density at the ith site given by $n_i(\epsilon_l) \equiv |\varphi_{l,i}|^2$. In Fig. 2(d) we show the i dependence of $n_i(\epsilon_l)$ for three different energy levels ϵ_l for $L = 50$: the chemical potential level ($l = L/2$), a slightly lower level ($l = 15$), and the band bottom ($l = 1$). For the original Hamiltonian, $n_i(\epsilon_l)$ does not depend on i, whereas SSD gives each position $\boldsymbol{r}_i$ its own energy scale proportional to $f_{\rm SSD}(\boldsymbol{r}_i)$. Consequently, the particles distribute in a way that forms a wave packet, which has a large weight at $\boldsymbol{r}_i$ that overall fulfills the relation $f_{\rm SSD}(\boldsymbol{r}_i) \sim |\epsilon_l|$; at $\epsilon_l \sim 0$, the wave function forms an edge state in which $f_{\rm SSD}(L/2) \sim 0$, whereas near the band edge with maximum $|\epsilon_l|$, the particle is localized at the center. Since $f_{\rm SSD} \sim 1$ at the system center [the shaded region in Fig. 2(d)], it is naturally expected that $n_c(\epsilon_l)$ is roughly the same as that for the original Hamiltonian. We therefore define an effective density of states (DOS) for system size L as

$$D_L(\epsilon_l) = \frac{2\bar{n}_c(\epsilon_l)}{\epsilon_{l+1} - \epsilon_{l-1}}, \tag{4}$$

where $\bar{n}_c(\epsilon_l) = n_c(\epsilon_{l+1})/4 + n_c(\epsilon_l)/2 + n_c(\epsilon_{l-1})/4$ is averaged over the neighboring three levels. Figure 2(b) shows $D_L(\epsilon)$ as vertical bars for a series of L, demonstrating that it agrees well with the exact 1D DOS, $D_{\rm 1D}(\epsilon) = (2\pi)^{-1}(1 - \epsilon^2/4)$, shown as solid lines, even for L as small as 4.

For the original Hamiltonian, $D_L(\epsilon)$ gives the conventional discrete DOS; since n_c is a constant filling factor of fermions, $D_L(\epsilon)$ is simply an inverse of the energy level spacings. Such a construction has a distinct difference from the SSD one; the SSD compresses the spacings between low-energy levels and at the same time redistributes the particle density at the system center in a way that suppresses n_c at low energies. These two effects result in $D_L(\epsilon)$ that well reproduces $D_{\rm 1D}(\epsilon)$.

These finding indicate that the particle density of the original Hamiltonian for $L \to \infty$ can be obtained from $n_c(\epsilon_l)$ equivalent to the fictitious DOS, $D_L(\epsilon_l)$,

$$\langle n(\mu, \beta)\rangle = \sum_{l=1}^{L} f(\epsilon_l) n_c(\epsilon_l), \tag{5}$$

where $f(\epsilon) = (e^{-\beta\epsilon} + 1)^{-1}$ is the Fermi distribution function. Due to the densely populated energy levels in the vicinity of the chemical potential, $\langle n(\mu, \beta)\rangle$ is nearly free of a size effect for $L \sim O(10)$. Let us consider an alternative expression in the many-body form. Construct a many-body wave function $|\psi_l(n_f)\rangle$ ($l = 1$ through Λ_{n_f}), with eigenenergy E_l, where Λ_{n_f} is the size of the Hilbert space for a given particle number n_f. One can easily confirm that the following form,

$$\langle n(\mu, \beta)\rangle = \frac{1}{\Xi_L} \sum_{n_f=0}^{L} \sum_{l=1}^{\Lambda_{n_f}} \langle \psi_l(n_f)|\hat{n}_c|\psi_l(n_f)\rangle e^{-\beta E_l}, \tag{6}$$

with $\Xi_N = \sum_{n_f,l} e^{-\beta E_l}$ exactly coincides with Eq. (5). This formula is equivalent to Eq. (3), with $\hat{A}_c = \hat{n}_c$.

2D Heisenberg systems. We apply our scheme to 2D systems. Figure 3(a) shows χ of the spin-1/2 square lattice Heisenberg antiferromagnet, in which we have chosen a system size of $N = 5 \times 5 = 25$ lattice. Here, since the TPQ method allows only a very small L in 2D, physical quantities oscillate as a function of $\boldsymbol{r}_i$ at $k_B T \lesssim 0.5$ due to boundary effects. As already known from the grand canonical analysis at $T = 0$, the center of oscillation is the true result we need to obtain [31]. The amplitude of oscillation depends on the choice of R. We tune the radius $R = R_0 + dR$ with dR

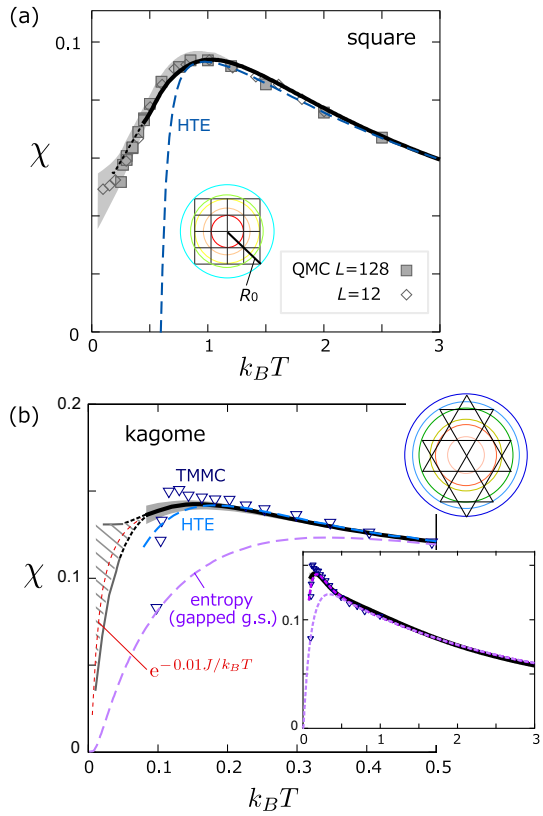

FIG. 3. Susceptibility χ of spin-1/2 2D Heisenberg models on (a) square and (b) kagome lattices of finite sizes and shapes shown in the insets, calculated with SSD, where the colored circles are a guide to the eye to clarify which sites and bonds belong to the same radius $\boldsymbol{r}_i$ in $f_{\rm SSD}(\mathrm{r_i})$. In each panel, the solid black line is our result, obtained for an optimal dR and making averages of ∼20 TPQ samples for (a), and ∼60 TPQ samples for (b). The shading at low T indicates uncertainties due to large spatial oscillations of $\langle m(\boldsymbol{r})\rangle$ near $\boldsymbol{r}=0$ that vary from TPQ sample to sample. The hatched region in (b) indicates the same ambiguity in our ED results, for which the 100 lowest states were used. Symbols and dashed lines indicate previous works: (a) QMC [13,41], HTE [42], and (b) TMMC [44], entropy method assuming a gap, $\Delta \sim 0.03J$ [19], HTE [46]. The lower inset to (b) shows our (as well as earlier) results to higher temperatures.

ranging from 0 to 1 to minimize such oscillations [39]. For each R, we make a 25 sample average of the initial TPQ states. The shaded region indicates the uncertainty due to the large oscillations that are inevitable at low T. For comparison, we also plot previous results of QMC calculations for $N = 128 \times 128$ [40] and 12×12 [13], and HTE [41,42], which is in agreement with our results, typically within $O(10^{-3})$ [43]. Here, the HTE provides a very useful check of the accuracy of our result for $k_BT \gtrsim 2$.

We finally present our unbiased susceptibility of the spin-1/2 antiferromagnetic Heisenberg kagome lattice in Fig. 3(b). It is widely studied by transfer-matrix Monte Carlo (TMMC) [44], NLC [45], HTE [17,46] with a Padé approximation, and entropy methods assuming gapped excitations [19,47]. Our result supports the strong enhancement at $k_BT \lesssim 0.5$, which is clearly seen in the inset. Previous results except for the one from the entropy method show a similar enhancement. Moreover, as shown in the main panel, our χ starts to drop at $k_BT \sim 0.1$, and is slightly smaller than the TMMC result. In this region, HTE is no longer reliable. At $k_BT < 0.1$ we have separately performed ED on $\mathcal{H}_{\rm SSD}$ for the lowest 100 states and evaluated the range of χ, indicated by hatching, in order to clarify whether the spin gap is finite or not. The range of hatching indicates the ambiguity arising from the large oscillation of $\langle m(\boldsymbol{r}_i)\rangle$ at $r_i \sim 0$, which increases at lower T. We plot $\chi \sim e^{-\Delta/k_BT}$, which is expected for the spin gapped system, and find that even if the gap were finite, it should be as small as $\Delta/J \sim 0.01$–0.02.

There are many ED studies on 2D quantum magnets that calculate χ and specific heat at $k_BT \lesssim 0.1$. However, at such low temperatures, finite-size effects become a serious problem. Our nearly size-dependence-free scheme also suffers from this limitation. Since our scheme is compatible with any numerical solver, it should be able to attack this extremely difficult temperature region once a powerful solver is developed that can handle twice as large a system than is currently possible.

Note added. Recently, we became aware of a related work on χ of the kagome lattice Heisenberg model by the finite-temperature Lanczos method at $N = 42$, consistent with our Fig. 3(b) [48].

Acknowledgments. We thank Johannes Richter and Laura Messio for useful discussions and Yasu Takano for giving us much advice. This work was supported by JSPS KAKENHI Grants No. JP17K05533, No. JP18H01173, No. JP17K05497, and No. JP17H02916.

[1] L. Balents, Nature (London) **464**, 199 (2010).
[2] S. Depenbrock, I. P. McCulloch, and U. Schollwöck, Phys. Rev. Lett. **109**, 067201 (2012).
[3] A. Kitaev, Ann. Phys. **321**, 2 (2006).
[4] J. S. Helton, K. Matan, M. P. Shores, E. A. Nytko, B. M. Bartlett, Y. Yoshida, Y. Takano, A. Suslov, Y. Qiu, J.-H. Chung, D. G. Nocera, and Y. S. Lee, Phys. Rev. Lett. **98**, 107204 (2007).
[5] F. Bert and P. Mendels, J. Phys. Soc. Jpn. **79**, 011001 (2010).
[6] Y. Okamoto, H. Yoshida, and Z. Hiroi, J. Phys. Soc. Jpn. **78**, 033701 (2009).
[7] Y. Shimizu, K. Miyagawa, K. Kanoda, M. Maesato, and G. Saito, Phys. Rev. Lett. **91**, 107001 (2003).
[8] Y. Yoshida, H. Ito, M. Maesato, Y. Shimizu, H. Hayama, T. Hiramatsu, Y. Nakamura, H. Kishida, T. Koretsune, C. Hotta, and G. Saito, Nat. Phys. **11**, 679 (2015).
[9] J. Jaklic and P. Prelovsek, Phys. Rev. B **49**, 5065(R) (1994).
[10] P. de Vries and H. De Raedt, Phys. Rev. B **47**, 7929 (1993).
[11] T. Iitaka and T. Ebisuzaki, Phys. Rev. Lett. **90**, 047203 (2003).
[12] S. Sugiura and A. Shimizu, Phys. Rev. Lett. **111**, 010401 (2013).
[13] Y. Okabe and M. Kikuchi, J. Phys. Soc. Jpn. **57**, 4351 (1988).
[14] C. Yasuda, S. Todo, K. Hukushima, F. Alet, M. Keller, M. Troyer, and H. Takayama, Phys. Rev. Lett. **94**, 217201 (2005).

[15] J. Oitmaa, C. Hamer, and W. Zheng, *Series Expansion Methods for Strongly Interacting Lattice Models* (Cambridge University Press, Cambridge, U.K., 2010).
[16] J. Oitmaa and E. Bornilla, Phys. Rev. B **53**, 14228 (1996).
[17] N. Elstner and A. P. Young, Phys. Rev. B **50**, 6871 (1994).
[18] M. Rigol, T. Bryant, and R. R. P. Singh, Phys. Rev. Lett. **97**, 187202 (2006).
[19] B. Bernu and C. Lhuillier, Phys. Rev. Lett. **114**, 057201 (2015).
[20] A. Gendiar, R. Krcmar, and T. Nishino, Prog. Theor. Phys. **122**, 953 (2009); **123**, 393 (2010).
[21] A. Gendiar, M. Daniska, Y. Lee, and T. Nishino, Phys. Rev. A **83**, 052118 (2011).
[22] T. Hikihara and T. Nishino, Phys. Rev. B **83**, 060414(R) (2011).
[23] H. Katsura, J. Phys. A: Math. Theor. **44**, 252001 (2011).
[24] K. Okunishi and H. Katsura, J. Phys. A: Math. Theor. **48**, 445208 (2015).
[25] C. Hotta, S. Nishimoto, and N. Shibata, Phys. Rev. B **87**, 115128 (2013).
[26] A. A. Belavin, A. M. Polyakov, and A. B. Zamolodchikov, Nucl. Phys. B **241**, 333 (1984).
[27] H. Katsura, J. Phys. A: Math. Theor. **45**, 115003 (2012).
[28] K. Okunishi, Prog. Theor. Exp. Phys. **2016**, 063A02 (2016).
[29] T. Tada, Mod. Phys. Lett. A **30**, 1550092 (2015).
[30] In two dimensions, we take $f_{\rm SSD}(\boldsymbol{r}_i)$, a radial function instead of the product of sine functions in two different directions, since it is shown to be more efficient at $T = 0$ in Ref. [32].
[31] C. Hotta and N. Shibata, Phys. Rev. B **86**, 041108(R) (2012).
[32] S. Nishimoto, N. Shibata, and C. Hotta, Nat. Commun. **4**, 2287 (2013).
[33] I. Maruyama, H. Katsura, and T. Hikihara, Phys. Rev. B **84**, 165132 (2011).
[34] S. Tamura and H. Katsura, Prog. Theor. Exp. Phys. **2017**, 113A01.
[35] The TPQ method [10–12] indicates a method that evaluates the finite-temperature physical properties by a few numbers of states with a reasonably small error. By repeatedly operating the Hamiltonian to an initial random vector, one can generate a series of pure states that represent thermal equilibrium states at various temperatures. The evaluations of the physical quantities are made by the canonical ensemble of these pure states. We prepared more than 20 initial random vectors, and made over 300 iterations to reach $k_B T \sim 0.01$.
[36] A. Klümper, Z. Phys. B **91**, 507 (1993); Eur. Phys. J. B **5**, 677 (1998); Lect. Notes Phys. **645**, 349 (2004).
[37] S. Eggert, I. Affleck, and M. Takahashi, Phys. Rev. Lett. **73**, 332 (1994).
[38] J. Cardy, *Scaling and Renormalization in Statistical Physics* (Cambridge University Press, Cambridge, U.K., 1996).
[39] See Supplemental Material at http://link.aps.org/supplemental/10.1103/PhysRevB.98.140405 for details of the following calculation: Taking $R = R_0 + dR$, dR ranging from 0 to 1, we evaluate the quantities of the center two sites and choose the one with the smallest oscillations at low T to extract the center of the oscillation. The oscillation of $\langle m(\boldsymbol{r}_i)\rangle$ is also found in the case of 1D at $L \sim 4$.
[40] M. S. Makivić and H.-Q. Ding, Phys. Rev. B **43**, 3562 (1991).
[41] J. Wang, Phys. Rev. B **45**, 2282 (1992).
[42] G. R. Rushbrooks, G. A. Baker, Jr., and P. J. Wood, in *Phase Transitions and Critical Phenomena*, edited by C. Domb and M. S. Green (Academic, New York, 1974), Vol. 3.
[43] In the grand canonical analysis in Refs. [25,30] using SSD, the best accuracy of the quantities of the 2D ground state was $O(10^{-3})$, which also holds for the present scheme. This accuracy allows us to evaluate most of the physical properties numerically.
[44] T. Nakamura and S. Miyashita, Phys. Rev. B **52**, 9174 (1995).
[45] M. Rigol and R. R. P. Singh, Phys. Rev. Lett. **98**, 207204 (2007).
[46] A. Lohmann, H.-J. Schmidt, and J. Richter, Phys. Rev. B **89**, 014415 (2014).
[47] The entropy method, when assuming gapless excitations in the kagome lattice Heisenberg model, will give χ compatible with our results; L. Messio, B. Bernu, K. Essafi, and L. Pierre (private communication).
[48] J. Schnack, J. Schulenburg, and J. Richter, Phys. Rev. B **98**, 094423 (2018).